Ibn Al-Haitham Journal for Pure and Applied Sciences
Journal homepage: jih.uobaghdad.edu.iq
PISSN: 1609-4042, EISSN: 2521-3407
IHJPAS. 2024, 37(3)

Synthesis and Characterization Two Nanocomposites of Fe_3O_4 Nnanoparticles and Using Them as a Chemical Sensors

Ameer Abdul Raheem Nemea[1*] and Basim I. Al-Abdaly[2]
[1,2]Department of Chemistry, College of Sciences, University of Baghdad, Baghdad, Iraq.
*Corresponding Author.

Received: 24 February 2023 Accepted: 30 March 2023 Published: 20 July 2024
doi.org/10.30526/37.3.3293

Abstract

The sensor aspect is one of the most critical disciplines due to its wide application in life. This work has studied the performance of the Fe_3O_4 nanocomposite, which was prepared by the synthesis of Fe_3O_4 nanoparticles (NPs) by the co-precipitation method through its precursors, which are ferric chloride and ferrous chloride. On the other hand, graphene oxide was synthesized using the Hummers method. Chemical sensing is a process that converts a chemical or physical change of a specific analyte into a measurable signal whose magnitude is usually proportional to the concentration of the analyte. The chemical sensor is an analyzer that responds to a particular analyte and reflects that response into an analytical electrical signal. The carbon nanotubes (CNTs) have been purchased to provide two matrixes (substrates) for nanocomposites. The sonication technique has been used to prepare the composites: the first nanocomposite is made of iron oxide NPs and graphene oxide NPs, and the second is made of iron oxide NPs with CNTs. Many techniques, such as AFM, SEM-EDX, FTIR, and XRD, have been used for characterization. There are specific factors indicated in the sensing, which are sensitivity, response time, and recovery time. In the Fe_3O_4/CNT nanocomposite state, the sensitivity is higher than that of Fe_3O_4/GO, and there is also a difference between them in response and recovery times. It has been observed that there was a difference between the two nanocomposites in the pattern of the cyclic voltammetry curve, with Fe_3O_4/CNTs being more regular than Fe_3O_4/GO for sensing glucose molecules.

Keywords: Nanocomposite, ferric oxide nanoparticles, gas sensor, biosensor, matrix, cyclic voltammetry.

1. Introduction

The chemical sensor is an analyzer that responds to a particular analyte and reflects that response into an analytical electrical signal. Although the chemical sensor topic has been a modern discipline, it has gained increasing attraction due to its applications in environmental monitoring, gas composition analysis, industrial processes, medicine, public contributed to by multidisciplinary studies like chemistry, biology, electricity, and semiconductor security, etc.,

and that returns to its attractive properties such as its small size, sound sensitivity, low cost, and ease of preparation and use. The chemical sensor topic was developed and technology principles, and the most common types are gas sensors for trace gas monitoring, ion sensors represented by the pH sensor, humidity sensors, and biosensors [1]. This work deals with gas sensors when using oxidizing NO_2 gas and biosensors when using glucose molecules in a particular electrolyte. The development trend of chemical sensors is linked with environmental protection and monitoring, and metal oxide nanoparticles (NPs) are typically used to prepare a sensor owing to their excellent sensitivity. Both gas and biological sensors played a pivotal role in many applications; their critical performance was based on the sensitivity of the target element [2]. The Fe_3O_4 NPs have been applied in biological and gas sensor fields because of their inexpensive fabrication process, low toxicity, high adsorption performance, and fast electron transfer capability [3]. They are an excellent sensing material and have been extensively studied because of their good characteristics, such as high sensitivity and good stability. Graphene oxide (GO) has been considered an exceptional candidate to develop the electrical conductivity of Fe_3O_4 NPs, thus the sensing applications, due to the following merits: (1) the two-dimensional honeycomb structure, which will quickly provide a high surface area and therefore high sensitivity to various materials (2) The high quality of the crystal lattice leads to low electric noise [4]. These merits help to improve the capturing and migrating of electrons between nanocomposites and tar Fe_3O_4 get material and could be used in carbon nanotubes (CNTs) for the same reason. The sol-gel method for Fe_3O_4 NPs is most suitable owing to the use of a small quantity of low-cost precursors, low temperature, and a simple synthesis technique [5]. Iron oxide exists in three forms in nature: magnetite (Fe_3O_4), maghemite (γ- Fe_3O_4), and hematite (α- Fe_3O_4). Actually, the crystalline iron oxide NPs were found with a mixture of magnetite and maghemite [6]. As mentioned before, chemical sensors can be used in different applications. In this work, we will consider the following two factors: 1) Gas sensing. In this study, CNTs and GO are compared while creating nanocomposites and employing them as sensors for the oxidizing gas NO_2. Gas sensing technology relies on tracking changes in the target material's direct resistance to adsorption and desorption [4]. Measures of gas sensing can be classified into a number of categories, including sensitivity, stability, selectivity, response, and recovery time [7]. The concentration of NO_2 gas on sensitivity will be between (80-100) ppm flow rate [8]. Heat it to various temperatures until it reaches the ideal temperatures; 2) Bio-sensing. All researchers who investigate biosensors share a similar interest in glucose biosensors because of the critical role they play in the treatment and management of diabetes. Recently, bio-applications of iron oxides have been attracting attention [9]. Due to their exceptional biocompatibility, super-paramagnetic characteristics, and electrical activity, Fe_3O_4 NPs are, in fact, regarded as suitable biosensors [10]. Cyclic voltammetry will be used in bio-sensing. An ITO conductive slide will be used, and after depositing nanocomposites on it with binding material (Nafion) and dipping in a specific electrolyte, this slide was connected to a cycle by using a platinum electrode to connect both sides of the electric circuit with a cyclic voltammetry device. Also, this sensing has been observed by gradually adding glucose [11].

2. Materials and Methods

2.1 Materials

In the present study, all materials from Sigma-Aldrich, including ferric chloride ($FeCl_3.6H_2O$) and its purity= 99.9%, for ferrous chloride ($FeCl_2$)= 98%, ammonium hydroxide (NH_4OH)= 25%, CNTs (C)= 98%, and for graphite (C)= 99.99%. The de-ionized water was from local markets.

2.2 Methods

2.2.1 Preparation of iron oxide Fe_3O_4 NPs by co-precipitation method

Iron chloride can be used as a precursor, and ammonium hydroxide can be used as a reducing agent to create iron oxide NPs quickly and efficiently (Shenmin *et al*., 2013). About 1.35 g of $FeCl_3.6H_2O$ and 0.5 g of $FeCl_2$ were dissolved in 50 mL of de-ionized water at 60^{o} C; after 30 minutes of proper mixing, 33 mL of ammonium hydroxide dropwise was added. Ammonium hydroxide dropwise was added to the mixture at room temperature to adjust the pH of the solution. After that, the solution's color turned black, which indicated that for the reduction process, the solution was left for 2 hours for proper mixing to complete reduction. After centrifuging the solution, it filtered out the black color, washed with de-ionized water and ethanol several times to remove the unwanted impurities, and dried, forming a black powder.

2.2.2 Preparation of graphene oxide NPs by hummer's method

About 1 g of graphite in 25 mL of sulfuric acid was put in an ice bath, vigorously stirring; 3 g of potassium permanganate was added very slowly, keeping the temperature below 20^{o}C, and stirring for 3 hours. Distilled water (50 mL) was added dropwise, keeping the temperature below 50^{o}C. After some time, the color of the colloidal changed to dark brown, indicating the formation of GO. Then, 100 mL of distilled water was added for complete oxidation. To stop the reaction, 5 mL of hydrogen peroxide was added carefully. After centrifuging, it is filtered out, washed several times with distilled water, and dried to get black powder [12].

2.2.3 Preparation of nanocomposites

Following the creation, as mentioned above, of Fe_3O_4 NPs, two nanocomposite materials will be made from this metal oxide, the first of which will contain GO and the second of which will contain CNTs. The ratio of the matrix mixture (GO or CNTs) to the metal oxide NPs was 2:8. The process for both nanocomposites involved placing metal oxide NPs (200 mg) in an appropriate volume of absolute ethanol and ultrasonically processing it for 20 minutes, followed by placing matrix material (800 mg) in a proper volume of deionized water and ultrasonically processing them for 30 minutes. Then, the two solutions were mixed vigorously for 20 minutes and transferred to ultrasonic for 30 minutes. The last steps were centrifuging and drying to get two black powders that represent two nanocomposites for the same Fe_3O_4 NPs but with different matrixes.

2.3 Chemical sensing techniques

2.3.1 Gas sensing technique

Before presenting the data for the NO_2 gas sensing, it must explain some factors of sense, like sensitivity (S), which is connected with the resistance (R) of the sensor (nanocomposites), because there is a difference in resistance when the flow of the gas (80–100 ppm) concentration is on and off. Then, the sensitivity was calculated according to the following relation and the other important factors in data are response and recovery times [7]:

$$\mathbf{S}\% = \frac{(\mathbf{R\ on} - \mathbf{R\ off})}{(\mathbf{R\ on})} \times 100\% \quad (1)$$

The response time was defined as the time to reach a 90% maximum value of conductance when using reducing gas or the minimum value of conductance when using oxidizing gas. On the other hand, the recovery time is the time required to recover within 10% of the original baseline when the flow of reducing or oxidizing gas was removed [8].

2.3.2 Bio-sensing technique

The sample was prepared to be examined through cyclic voltammetry by following the steps [15]:

- About 20 μm from Nafion (binding material), 25 mL of ethanol, and 25 mL of de-ionized water were added to a beaker containing 100 mL of nanocomposite and let under sonication for (10-15) minutes using an ultrasonic cleaner.
- Then, a piece of the slide (ITO) was put on a hot plate, and a mixture (already prepared) was precipitated drop by drop until the precipitation was completed, using a pipette.
- The electrolyte in question was prepared from 10 mL of (0.1 M) NaOH in distilled water at a scan rate of 50 $mV.S^{-1}$.
- The amperometric responses to the successive additions of glucose concentration in the solution were at +0.13V (VS. Ag/AgCl).
- About 10 mL of 0.1 M glucose solution was prepared and added millimeter after millimeter for each cycle of the cyclic voltammetry and the change on screen was observed using platinum electrodes.

3. Results

3.1 Characterization of Fe_3O_4/GO and Fe_3O_4/CNT nanocomposite

Firstly, the nanoscale of Fe_3O_4 was insured through AFM images before the preparation of each nanocomposite. The AFM (2D and 3D) image showed that the surface morphology was not smooth and had agglomerated particles, which are represented by the white peaks. This aggregation can be caused by the measurement method [13]. The average diameter of Fe_3O_4 NPs was 31.27 nm, GO NPs was 63.94 nm, and CNTs was 43.5 nm [14, 15], as shown in **Figures 1** and **2** .

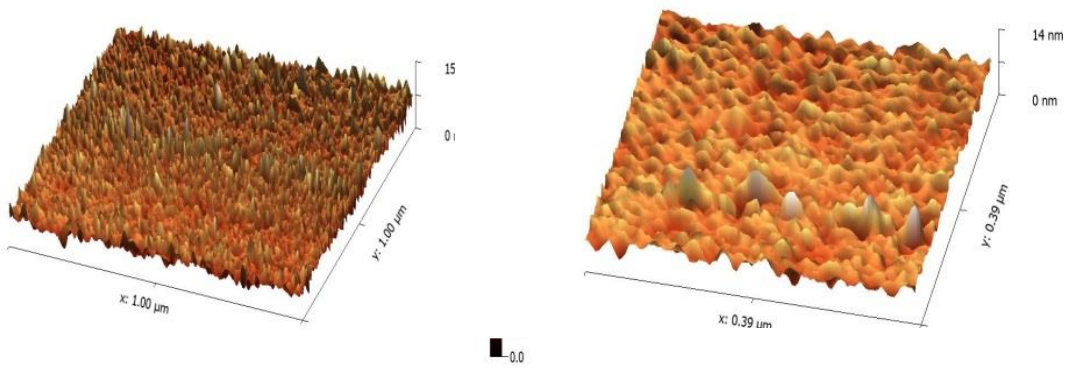

Figure 1. The AFM images (2D and3D) of Fe_3O_4 NPs.

3.1.1 The SEM-EDX for Fe_3O_4/GO

There is a distribution of iron (spinal) oxide NPs on the surface of GO, as the SEM technique shows, and the components of nanocomposites are (C) 51.2%, (O) 15.4%, and (Fe) 33.4% [13,14], as EDX shows in **Figure 2**.

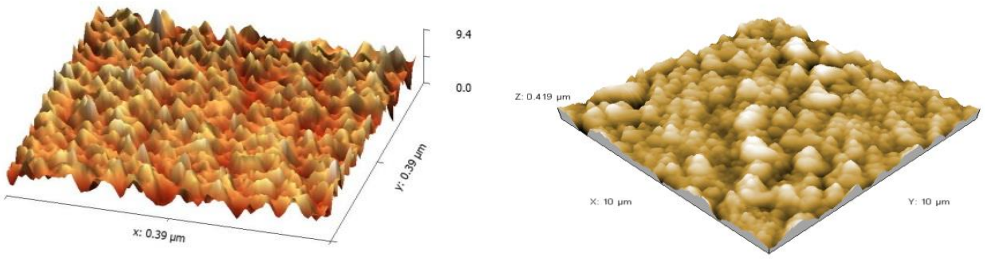

A B

Figure 2. The AFM images (2D and3D) of A: GO NPs and B: CNTs.

3.1.2 The FTIR for Fe_3O_4/GO

The results of the FT-IR spectrum of Fe_3O_4 / GO showed there is a reaction between the (O-H) groups of Fe_3O_4/GO at 1604.66 cm^{-1}, which is ascribed to the (H-O-H) bending mode. The peak at 1344.29 cm^{-1} is referred to as (C-O) stretching, 1099 cm^{-1} is for (H-O-Fe) stretching, and 611.39 cm^{-1} and 567 cm^{-1} are referred to as (Fe-O) bonds [13, 14], as shown in **Figure 3**.

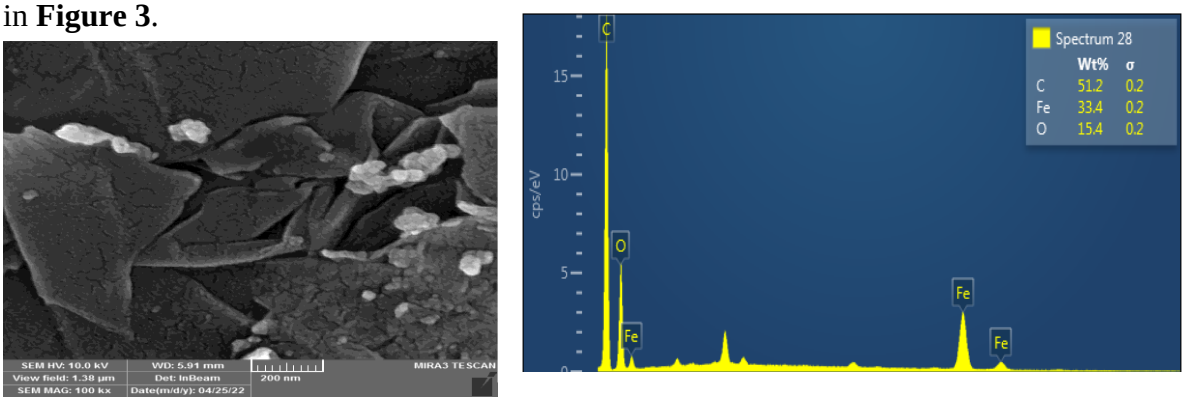

Figure 3. The SEM and EDX images of Fe_3O_4/ GO nanocomposite.

3.1.3 The XRD for Fe_3O_4/GO

Through treatment of the data in the Origin Pro 8 program, we have obtained the following data: FWHM was (1.69387) and 2 thetas were 26.46259, and after using those values with Scherrer equation, take a piece from the plot having the highest peaks and do analysis for them to get crystallite size equal to (16 nm), and by entering the data [13, 14], the plot was drawn as in **Figure 4**.

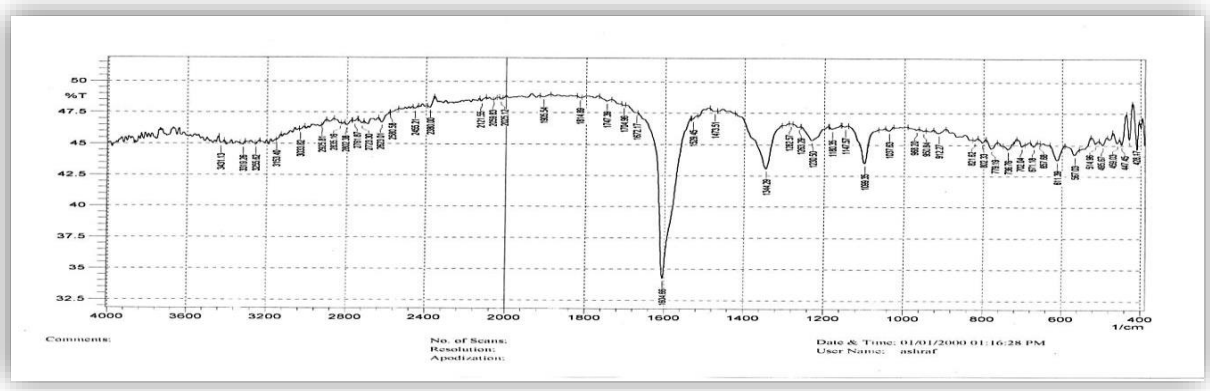

Figure 4. The FT-IR spectrum for Fe_3O_4/ GO nanocomposite.

3.1.4 The SEM-EDX for Fe_3O_4/CNT

There was a distribution of iron (spinal) oxide NPs on the surface of CNTs, as the SEM technique shows, and the components of nanocomposites are (C) 86.9%, (O) 8.3%, and (Fe) 4.8% [13, 14], as in **Figure 5**.

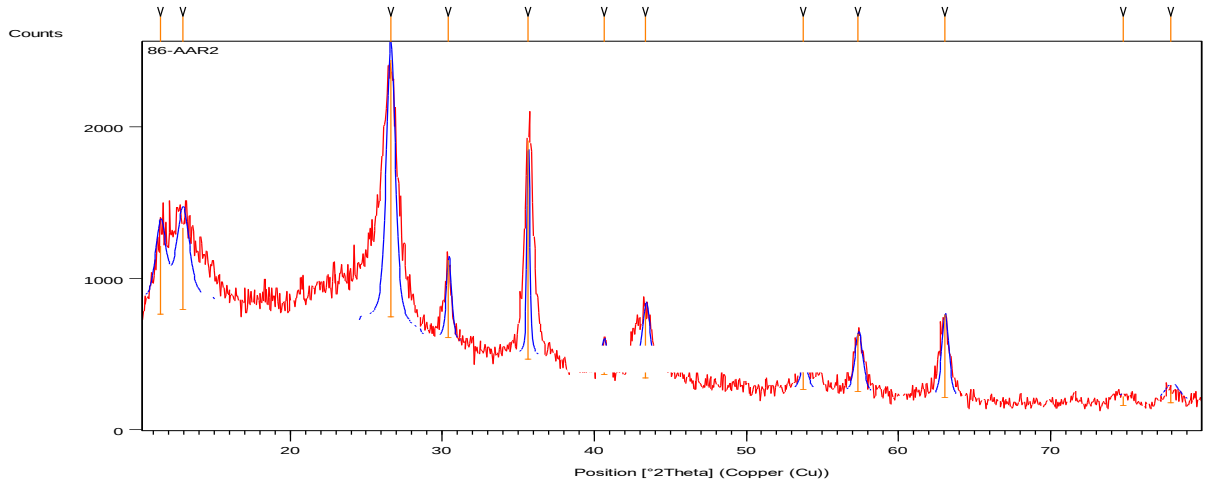

Figure 5. The XRD pattern of Fe_3O_4/GO nanocomposite.

3.1.5 The FTIR for Fe_3O_4/CNT

The results of the FT-IR spectrum of Fe3O4 and CNT showed a band at 3500.56 cm^{-1} to 3429.20 cm^{-1} attributed to the (O-H) of H_2O molecules that were interlayers of composites, and there were weak peaks at 2921.96 cm^{-1} and 2850.59 cm^{-1} ascribed to the (C-H) of organic residues. There is a peak at 1614.31 cm^{-1} is ascribed to the (C=O) group, and the peak at 1367.44 cm^{-1} is referred to as (C-O) stretching, 1097.42 cm^{-1} as (H-O-Fe) stretching, and 617.18 cm^{-1} to 445.53 cm^{-1} were referred to as (Fe-O) bond [13, 14], as shown in **Figure 6**.

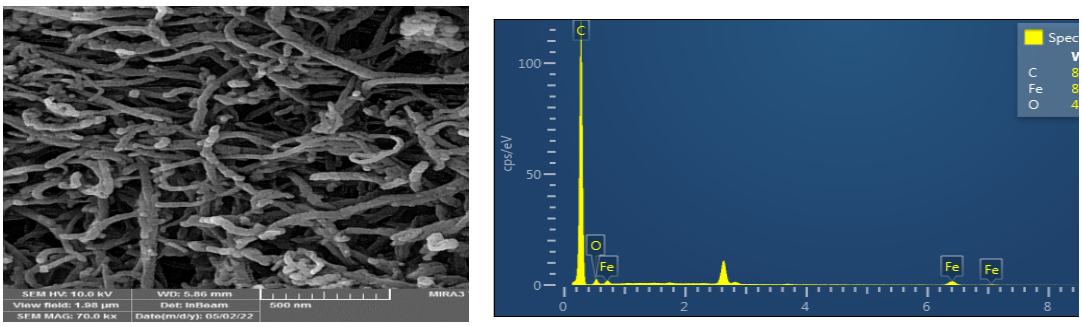

Figure 6. The SEM and EDX images of Fe_2O_3 / CNT nanocomposite.

3.1.6 The XRD for Fe_3O_4/CNT

Through treatment of the data in the Origin Pro 8 program, it obtained the following data: FWHM was (1.14111) and 2 theta was 26.41637. After using those values with the Scherrer equation, taking a piece from the plot having the highest peaks, and analyzing them, it was obtained that the crystallite size equals (9 nm). By entering the data [13, 14], it obtained the plot as in **Figure 7**.

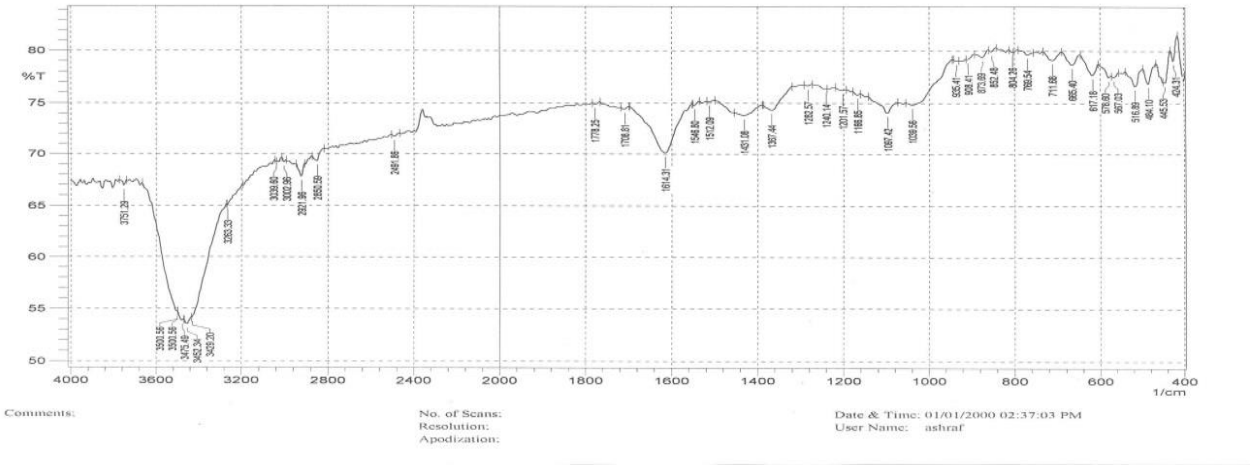

Figure 7. The FT-IR spectrum of Fe_3O_4/ CNT nanocomposite.

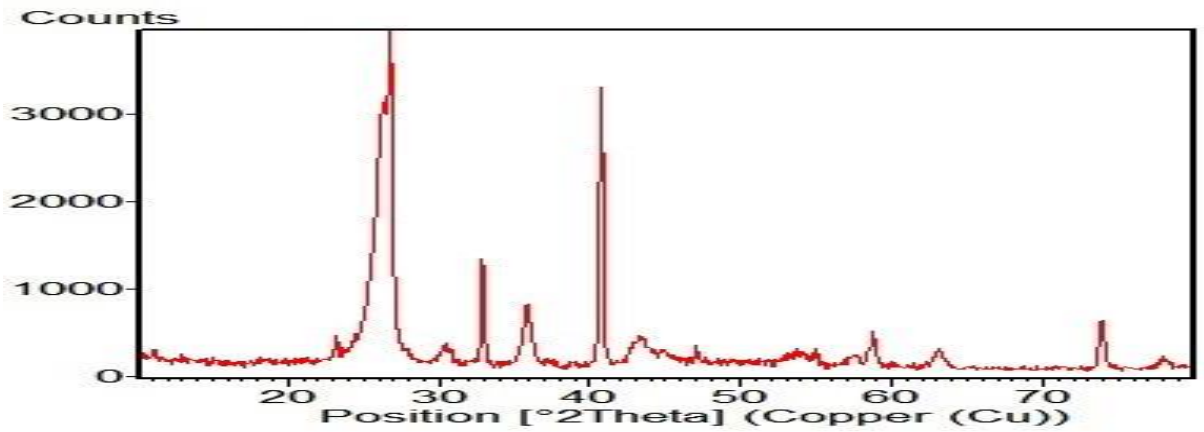

Figure 8. The XRD pattern of Fe_3O_4/CNT nanocomposite.

3.2 Gas sensing data

3.2.1 The data sensing of Fe_3O_4/GO nanocomposite

Series (1) refers to the relationship between a response time and temperature, and series (2) refers to the relationship between a recovery time and temperature [16, 23]. To summarize the data of Fe_3O_4/GO nanocomposites (sensors) for the different temperatures (25, 80, 130, and 200) °C as shown in **Table 1**.

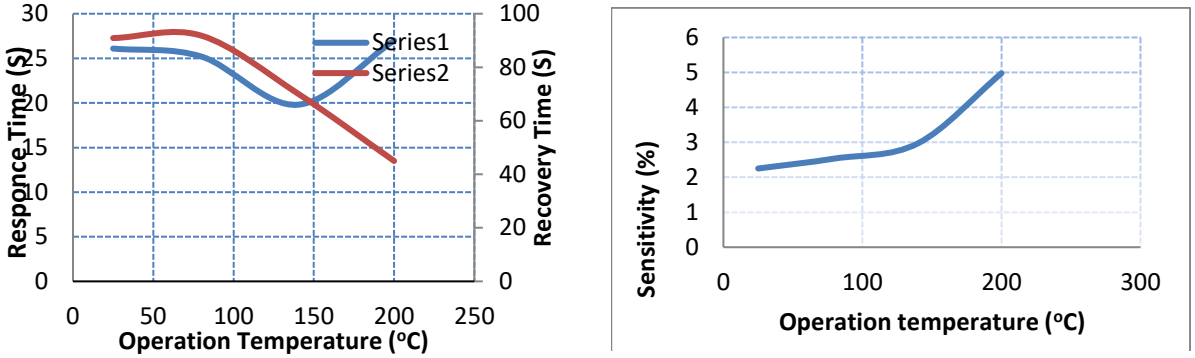

Figure 9. Sensing plots of Fe_3O_4/GO nanocomposite.

Table 1. The data of Fe_3O_4/GO nanocomposite for NO_2 sensing.

No.	Temperature (°C)	Sensitivity (S%)	Response time (sec.)	Recovery time (sec.)
1	25	2.251	26.1	90.9
2	80	2.536	25.2	91.8
3	130	2.971	19.8	70.2
4	200	4.975	27	45

3.2.2 The data sensing of Fe_3O_4/CNT nanocomposite

Figure 10 reveals the sensing plots of Fe_3O_4/CNT nanocomposite. The data of Fe_3O_4/CNT nanocomposite for NO_2 sensing are illustrated in **Table 2**.

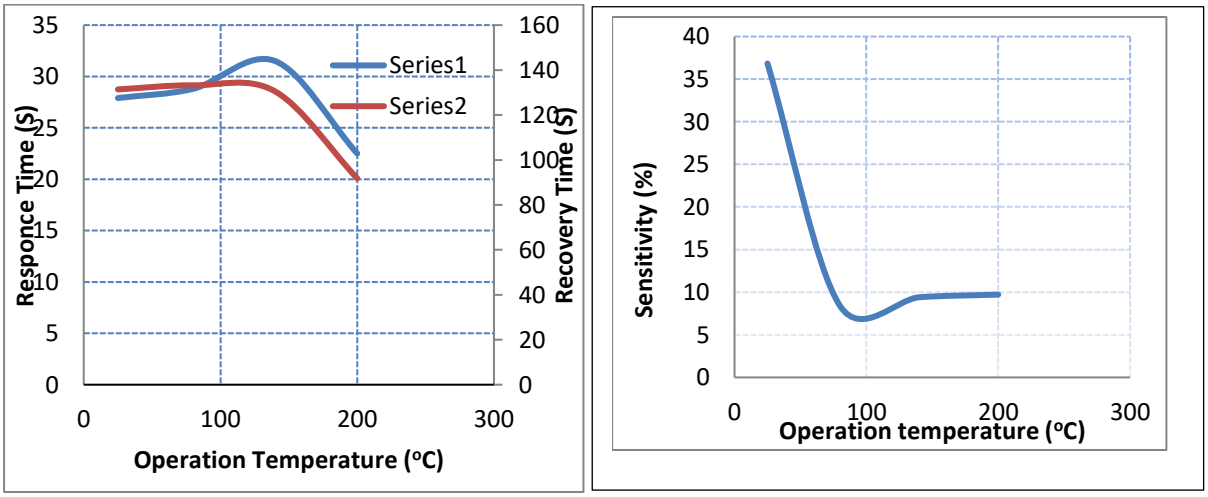

Figure 10. Sensing plots of Fe_3O_4/CNT nanocomposite.

Table 2. The data of Fe_3O_4/CNT nanocomposite for NO_2 sensing.

No.	Temperature (°C)	Sensitivity (S%)	Response time (sec.)	Recovery time (sec.)
1	25	36.84	27.9	131.4
2	80	8.39	28.8	133.2
3	130	9.40	31.5	130.5
4	200	9.72	22.5	91.8

3.3 Bio sensing results

By cyclic voltammetry [17, 18, 24], the resulting data of the two nanocomposites (Fe_3O_4/GO and Fe_3O_4/CNT) as biosensors have been obtained as follows:

3.3.1 Fe_3O_4/GO nanocomposite

Leaner increasing but not regular, as shown in **Figure 10**.

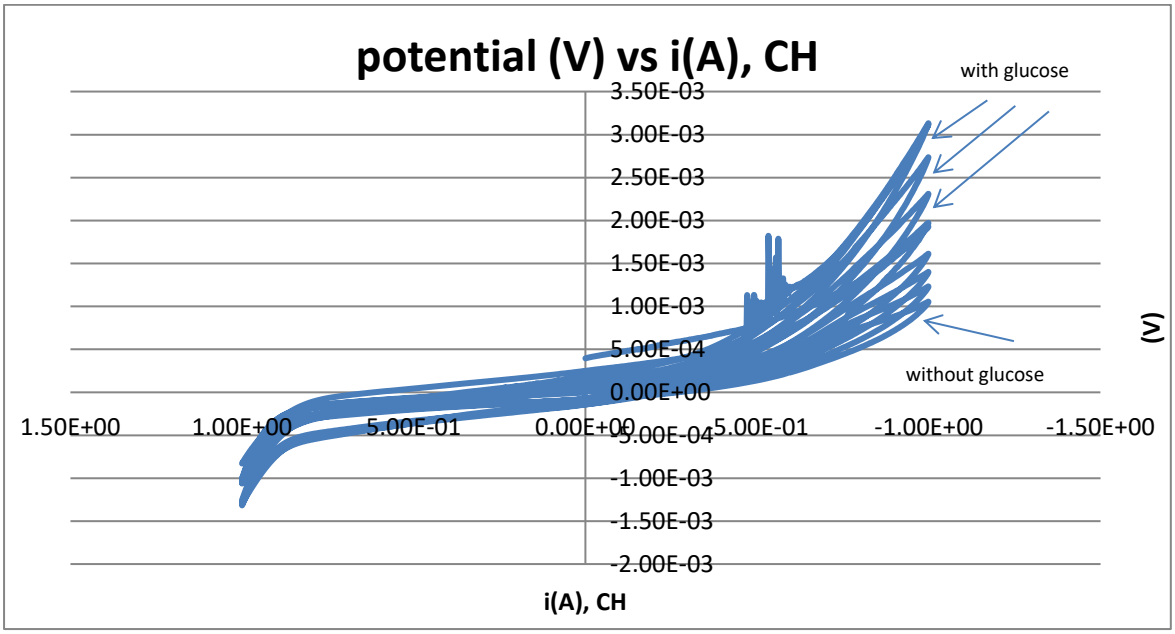

Figure 10. The bio-sensing chart of glucose using Fe_3O_4 / GO nanocomposite.

3.3.2 Fe_3O_4/CNT nanocomposite

Linear and regular increasing, as shown in **Figure 11**.

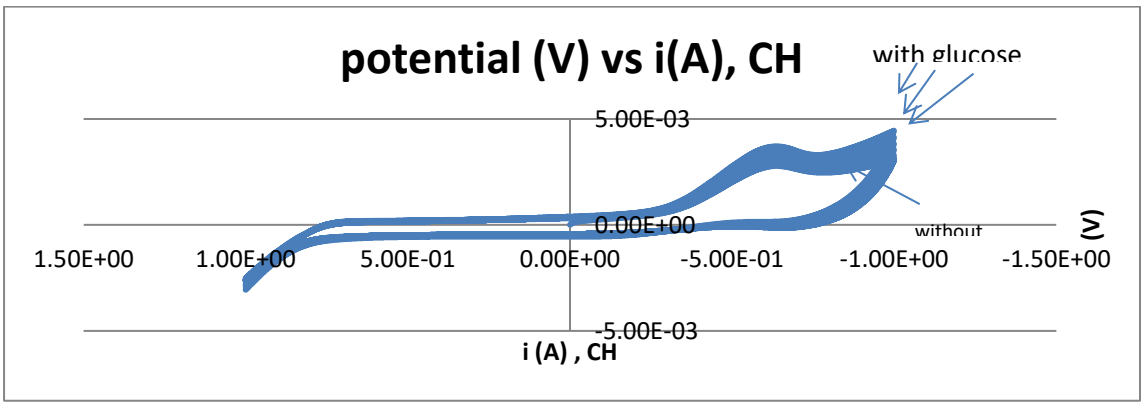

Figure 11. The bio-sensing chart of glucose using Fe_3O_4/CNT nanocomposite.

4. Discussion

The main goal of this work is to study the data of sensing, whether in gas-sensing or bio-sensing, for the same metal oxide Fe_3O_4 when using it with different matrixes (substrates) to form two different nanocomposites [19,25]. When studying the data of the results for two nanocomposites, it was observed that the surface of each of them was different. The GO-based composite surface was made of plates or sheets, as shown in **Figure 3**. Still, the CNT-based composite surface was as tubes in **Figure 6**.

In EDX images, it was observed that the proportion of (C) (86.9%) in CNTs-based composites was higher than the proportion of (C) (51.2%) in GO-based composites that return to the nature of the matrix. The high proportion of (C) in CNTs-based nanocomposite reflected the presence of a (C-O) bond in the FTIR, which had a somewhat weak peak but was clearer in Fe_3O_4/GO than in Fe_3O_4/CNTs. The XRD was observed in the Fe_3O_4/GO pattern, which contains more peaks than the Fe_3O_4/CNTs pattern; furthermore, the crystalline size of the Fe_3O_4/GO nanocomposite was (36.178 nm) and that of the Fe_3O_4/CNTs was (6.267 nm) respectively [20, 26]. The difference has been observed in two techniques: in gas sensing data, the sensitivity of Fe_3O_4/CNT is higher than that of Fe_3O_4/GO, and observing the same thing when comparing response and recovery times, as has been written in the two **Tables** above [21, 27, 28].

In bio-sensing, the difference between two nanocomposites in their regularity could be seen, although both of them sensed the glucose in the electrolyte. However, with Fe_3O_4/CNT, the increase of sensing was regular, as in the chart above, but with Fe_3O_4/GO, it was irregular. It could be said that the chief reason for these differences in data in both techniques with two nanocomposites is the difference in matrixes (substrates) [22, 29, 30].

5. Conclusion

The final result of this work is to try to highlight the real reason for the difference in sensing between Fe_3O_4/GO nanocomposite and Fe_3O_4/CNT nanocomposite when using both of them as chemical sensors. After studying their data in two techniques, gas-sensing and bio-sensing, with the same circumstances and apparatus of sense, it could be concluded that the chief reason for that difference is a matrix (substrate). When using CNTs with nanocomposite, the gas sensing data showed high sensitivity and was more regular in the sensing of glucose. Therefore, to improve the capability of the sensor, one should choose the optimal matrix (substrate), which will enhance the electroactivity of the nanocomposite and, ultimately, the sensing behavior.

Acknowledgment

The authors thank the Department of Chemistry, College of Science, University of Baghdad, and Dr. Fwad Tariq Ibrahim in the Department of Physics, College of Science, University of Baghdad, and the Nano Technological Research Center at the University of Technology.

Conflict of Interest

The authors declare that they have no conflicts of interest.

Funding

The authors declare that they have no conflicts of interest.

Ethical Clearance

Ethics of scientific research were carried out in accordance with the international conditions followed in dealing with laboratory animals. These included animal health, husbandry and care for them, and providing appropriate conditions for them in terms of food. Appropriate methods were adopted in dealing with them when experimenting, and this is consistent with the instructions of the Iraqi Ministry of Health and Environment.

References

1. Janata. Introduction: modern topics in chemical sensing. *Chemical Reviews* **2008**, *108*(*2*), 327–328. https://doi.org/10.1021/cr0680991
2. Yong, S.K.; Ha, S.C.; Kim, K.; Yang, H. Room-Temperature Semiconductor Gas Sensor Based on Nonstoichiometric Tungsten Oxide Nanorod Film. *Applied Physics Letters* **2005**, *86*(*21*), 213105. doi: https://doi.org/10.1063/1.1929872
3. Suhanto, R.N.; Harimurti, S.; Septiani, N.L.W.; Utari, L.; Anshori, I.; Wasisto, H.; Suyatman, H.S.S; Yuliarto, B.; Sonochemical. Synthesis of Magnetic Fe_3O_4/ Graphene Nanocomposites for Label-Free Electrochemical Biosensors.. *Journal of Materials Science: Materials in Electronics* **2020**, *31*,15381–15393. https://doi.org/10.1007/s10854-020-04102-2.
4. Yang, Y.; Sun, L.; Dong, X.; Yu, H.; Wang, T.; Wang, J.; Wang, R.; Yua, W.; Liu, G. Fe_3O_4/rGO Nanocomposite: Synthesis and Enhanced Nox Gas-Sensing Properties At Room Temperature. *RSC Advance* **2016**, *43(6)*, 37085-37092. https://doi.org/10.1039/C6RA02306A.
5. Kayani, Z.N.; Arshad, S.; Riaz, S.; Naseem, S. Synthesis of Iron Oxide Nanoparticles by Sol–Gel Technique and Their Characterization. *IEEE Transactions on Magnetics* **2014**, *50*(*8*), 1-4. https://doi.org/10.1109/TMAG.2014.2313763
6. Ozel, F.; Kockar, H. ; Karaagac, O. Growth of Iron Oxide Nanoparticles by Hydrothermal Process: Effect of Reaction Parameters on the Nanoparticle Size. *Journal of Superconductivity and Novel Magnetism* **2015**, *28*, 823–829. https://doi.org/10.1007/s10948-014-2707-9
7. Yang, L.; Ren, X.; Tang, F.; Zhang, L. Practical Glucose Biosensor Based On Fe_3O_4 Nanoparticles And Chitosan/Nafion Composite Film. *Biosensors and Bioelectronics* **2009**, *25*(*4*), 889-895. https://doi.org/10.1016/j.bios.2009.09.002
8. Vinh, N.T.; Tuan, L.A.; Vinh, L.K.; Quy, N.V. Synthesis, characterization, and gas sensing properties of Fe_3O_4/FeOOH nanocomposites for a mass-type gas sensor. *Materials Science in Semiconductor Processing* **2020**, *118*©, 105211. https://doi.org/10.1016/j.mssp.2020.105211
9. Iwasakia, T.; Mizutania, N.; Watanoa, S.; Yanagidab, T.; Kawai, T. Hydrothermal synthesis of magnetite nanoparticles via sequential formation of iron hydroxide precipitates. *Journal of Experimental Nanoscience* **2012**, *7*(*4*), 355–365. https://doi.org/10.1080/17458080.2010.515250
10. Shenmin Zhu; Jingjing Guo; Junping Dong; Zhaowen Cui; Tao Lu; Chenglin Zhu; Di Zhang; Jun Mac; Sonochemical fabrication of Fe_3O_4 nanoparticles on reduced graphene oxide for biosensors. *Ul trasonics Sonochemistry* **2013**, *20*, 872–880. https://doi.org/10.1016/j.ultsonch.2012.12.001.
11. AL-Mokaram, A.M.A.; Yahya, R.; Abdi, M.M.; Mahmud, H.N.M.E. The Development of Non-Enzymatic Glucose Biosensors Based on Electrochemically Prepared Polypyrrole–Chitosan–Titanium Dioxide Nanocomposite Films. *Nanomaterials* **2017**, *7(6)*, 129. https://doi.org/10.3390/nano7060129.
12. Koli, P.B.; Birari, M.D.; Ahire, S.A.; Shinde, S.G.; Ingale, R.S.; Patil, I.J. Ferroso-Ferric Oxide (Fe_3O_4) Embedded G-C_3N_4 Nanocomposite Sensor Fabricated by Photolithographic Technique for

Environmental Pollutant Gas Sensing and Relative Humidity Characteristics. *Inorganic Chemistry Communications* **2022**, *146(7)*, 110083. https://doi.org/10.1016/j.inoche.2022.110083.

13. Alwash, A. The Green Synthesize of Zinc Oxide Catalyst Using Pomegranate Peels Extract for the Photocatalytic Degradation of Methylene Blue Dye. *Baghdad Sci. J.* **2020**, *17*(*3*), 787-794. https://doi.org/10.21123/bsj.2020.17.3.0787.
14. Zhu, Sh.; Guo, J.; Dong, J.; Cui, Z.; Lu, T.; Zhu, C.; Zhang, D.; Mac, J. Sonochemical Fabrication of Fe_3O_4 Nanoparticles on Reduced Graphene Oxide for Biosensors. Ultrasonics Sonochemistry **2013**, *20(3)*, 872-880. https://doi.org/10.1016/j.ultsonch.2012.12.001.
15. Suhanto, R.N.; Harimurti, S.; Septiani, N.L.W. Sonochemical synthesis of magnetic Fe_3O_4/ graphene nanocomposites for label-free electrochemical biosensors. *Journal of Materials Science: Materials in Electronics.* **2020**, *31*, 15381–15393. https://doi.org/10.1007/s10854-020-04102-2.
16. Al-Husseini AH, Saleh WR, Al-Sammarraie AMA; A Specific NH3 Gas Sensor of a Thick MWCNTs-OH Network for Detection at Room Temperature. *Journal of Nano Research.* **2019**, *56*, 98–108. https://doi.org/10.4028/www.scientific.net/JNanoR.56.98.
17. Hassan, T.A.A.; Al-Sammarraie, A.M.A. Growth of Different Zinc Oxide Nanostructures for Hydrogen Gas Sensing. *Journal of Global Pharma Technology* **2019**, *11*(*2*), 419-425. https://doi.org/10.21123/bsj.2023.8336.
18. Elewi, A.S.; Wadood, S.A.; Mohammed, A.M. Development of Hydrogen Peroxide Biosensor Based on Immobilization of Hemoglobin on Screen-Printed Carbon Electrode Modified with Silver Nanoparticles. *Iraqi Journal of Science.* **2019**, *60*(*11*), 2332-2340. https://doi.org/10.24996/ijs.2019.60.11.3.

Elewi, A.S.; Al-Shammaree, S.A.; AL Sammarraie, A.M.A. Hydrogen Peroxide Biosensor Based on Hemoglobin-Modified Gold Nanoparticles–Screen Printed Carbon Electrode. *Sensing and Bio-Sensing Research* **2020**, *28(9)*, 100340. https://doi.org/10.1016/j.sbsr.2020.100340.

20. Ulwall, R.A.; Abbas, H.K.; Karam, A.J.; Al-Zuky, A.A.; Al-Kadhemy, M.F.H.; Al-Saleh, A.H. Surface Plasmon Resonance (SPR) Simulation of a Gold-Bismuth Bi-layer Gas Sensor. *Iraqi Journal of Science* **2022**, *63*(*8*),3402-3411. https://doi.org/10.24996/ijs.2022.63.8.16.
21. Khamees, H.A.; Abid, M.A. Green Synthesis of IONPs for Photocatalytic Activities. *Ibn AL-Haitham Journal For Pure and Applied Sciences.* **2022**, *53(4)*, 125-135. https://doi.org/10.30526/35.4.2886.
22. Jihad, G.H. Synthesis and Characterization of α-Fe_2O_3Nanoparticles Prepared by PLD at Different Laser Energies. *Iraqi Journal of Science* **2021**, *62*(*11*), 3901-3910. https://doi.org/10.24996/ijs.2021.62.11.11
23. Mahmoud, Z.H.; Abdalstar, O.D.; Sabah, N. Semiconductor Metal Oxide Nanoparticles: A Review for the Potential of H_2S Gas Sensor Application. *Earthline Journal of Chemical Sciences* **2020**, *4(2)*, 199-208. https://doi.org/10.34198/ejcs.4220.199208.
24. Junior, R.A.; Alves, H.P.A.; Cartaxo, J.M.; Rodrigues, A.M.; Neves, G.A.; Menezes, R.R. Use of nanostructured and modified TiO_2 as a gas sensing agent. *Cerâmica* **2021**, *67* (*383*), 316-326. https://doi.org/10.1590/0366-69132021673833128.
25. Abed, G.M.; Al-Abdaly, B.I.; Alsammarraie, A.M.A. Low Temperature Hydrothermal Synthesis of Cu-Nd Doped Zinc Oxide Nanorods. *Iraqi Journal of Science.* **2016**, Part A, pp:1-10.
26. Abu-Hani, A.F.S.; Awwad, F.; Greish, Y.E.; Ayesh, A.I.; Mahmoud, S.T. Design, Fabrication, and Characterization of Low-Power Gas Sensors Based on Organic-Inorganic Nano-Composite. *Organic Electronics.* **2017**, *42* , 284-292. https://doi.org/10.1016/j.orgel.2016.12.050.
27. Pisarkiewicz, T.; Maziarz, W.; Małolepszy, A.; Stobinski, L.; Micho´n, D.; Rydosz, A. Multilayer Structure of Reduced Graphene Oxide and Copper Oxide as a Gas Sensor. *Coatings.* **2020**, *10(11)*,1015. https://doi.og/10.3390/coatings10111015.

28. Junhui, Xu.; Yazhen, Wang; Shengshui, Hu. Nanocomposites of graphene and graphene oxides: Synthesis,molecular functionalization and application in electrochemical sensors and biosensors A review. *Microchimica Acta.* **2017**, *184*(*1*),44. https://doi.org/10.1007/s00604-016-2007-0.
29. Kaushik, A.; Kumar, R.; Arya, S.K.; Nair, M.; Malhotra, B.D.; Bhansali, S. Organic–Inorganic Hybrid Nanocomposite-Based Gas Sensors for Environmental Monitoring. *Chemical reviews* **2015**, *115*(*11*), 4571–4606. DOI: https://doi.org/10.1021/cr400659h
30. Sarmed Salih Al-Awadi; Amer A. Ramadhan; Fuad T. Ibrahim; Ali K Abbood. Optical and Structural Properties of Titanium Dioxide Papered by DC Magneto-Sputtering as a NO_2 Gas Sensor. *Iraqi Journal of Science* **2020**, *61*(*10*), 2562-2569. https://doi.org/10.24996/ijs.2020.61.10.12.